*Bull. Mater. Sci.* (2020) 43:61
https://doi.org/10.1007/s12034-020-2043-6



# Thin film chemiresistive gas sensor on single-walled carbon nanotubes-functionalized with polyethylenimine (PEI) for $NO_2$ gas sensing

**SUNIL KUMAR[1,4,*], VLADIMIR PAVELYEV[1], PRABHASH MISHRA[1,2,3] and NISHANT TRIPATHI[1]**

[1]Department of Nanoengineering, Samara National Research University, Samara 443086, Russia
[2]Center for Photonics and 2D Materials, Moscow Institute of Physics and Technology (MIPT), Dolgoprudny 141700, Russia
[3]Centre for Nanoscience and Nanotechnology, Jamia Millia Islamia (Central University), New Delhi 110025, India
[4]ISOM, E.T.S.I. Telecommunication, Universidad Politecnica de Madrid, Madrid 28040, Spain
*Author for correspondence (sunil.kr.rai@outlook.com)

MS received 3 July 2019; accepted 17 November 2019; published online 10 February 2020

**Abstract.** Chemical detection of toxic gases, such as greenhouse gases is still very important as a research topic. To design gas sensor detectors based on single-walled carbon nanotubes (SWCNTs) with high sensitivity and selectivity for the toxic environment is a continuous process. The aim is to detect $NO_2$ gas with better sensitivity. In the present work, the thin-film sensor is fabricated on $SiO_2$ substrate and it is functionalized with polyethylenimine (PEI). It has been established that PEI functionalized SWCNTs (F-SWCNTs) show high sensitivity towards strong electron-withdrawing particles. It was found that at room temperature, SWCNTs-PEI functionalized gas sensor exhibited a higher sensitivity of 37.00% as compared with bare SWCNTs gas sensor. The gas sensor has shown the repeatable response for the entire concentration range studied. The sensing properties and the PEI functionalization duration effects on the behaviour of SWCNTs-based gas sensors were demonstrated.

**Keywords.** Carbon nanotubes; polyethylenimine (PEI); sensor; $NO_2$.

## 1. Introduction

The world health organization (WHO) 2016 report suggests that the 90% population of the world inhales the polluted air and is polluted beyond the limits specified by the WHO. The major components of this polluted air are nitrogen dioxide ($NO_2$), sulphur dioxide ($SO_2$), ozone ($O_3$), carbon monoxide (CO), volatile organic compounds (VOCs) and particulate matter (PM) [1]. Owing to globalization and rapid growth in the human population, there is a tremendous increase in the concentration of different greenhouse gases like $CO_2$, $H_2S$, $H_2O$ and $NO_2$, which leads to various respiratory diseases [2]. Although all of these gases are noxious to humans and to the environment, but the most crucial is the increase in the consolidation of toxic $NO_2$ gases. The overexposure of $NO_2$ in small concentration causes irritation in the human respiratory tract and in large concentration may lead to pulmonary disease and in the extreme case can cause loss of human life [3]. It can also cause a change in the blood composition, in particular, reduces the content of haemoglobin in blood [4]. The main source of the $NO_2$ gases is traffic and fossil fuel consumption processes. We can feel the presence of $NO_2$ gas when the concentration is 0.23 mg $m^{-3}$, but its adverse effect can be observed in healthy individual at the concentration of 0.056 mg $m^{-3}$, which is four times lower than the detection threshold. The people with chronic lung disease experience difficulty in breathing even at the concentration of 0.038 mg $m^{-3}$ $NO_2$ gases. Therefore, the detection to reduce the concentration of $NO_2$ under an ambient condition at room temperature is of great importance.

Conventional sensing material, such as metal oxide semiconductors have poor sensitivity at room temperature and requires an additional power supply source and microfabrication techniques for the normal functioning of the sensor. Some examples of metal oxide semiconductor-based $NO_2$ gas sensors are titanium dioxide ($TiO_2$), zinc oxide (ZnO), copper (II) phthalocyanine (CuPc) [5] and copper oxide (CuO) [6]. Metal oxide semiconductors-based gas sensors have been extensively used, but for particular detectors, the high operating temperature has restricted the development of such sensors because it requires high cost as well as the complicated configurations [7,8].

On the other hand, carbon nanotubes (CNTs) are one-dimensional (1-D) nanomaterial, which attract more consideration because they have high sensitivity for gases at room temperature [9,10]. It has been found that CNTs; are encouraging detecting material, which retains electrical properties and is extremely responsive to a low concentration of gases,

such as carbon dioxide ($CO_2$), nitrogen oxide ($NO_x$) and ammonia ($NH_3$) at room temperature. Besides, CNTs as ultra-sensitive sensing materials, also outperform the conventional sensing material, such as metal oxide semiconductor in terms of vast assimilative capability, large surface-area-to-volume ratio, low weight and rapid response time, resulting in momentous variations in electrical properties, such as resistance and capacitance [11,12]. After the breakthrough of CNTs by Iijima [13], CNTs have shown great potential and emerged as one of the most promising materials for a wide range of engineering applications, such as optoelectronics [14,15], sensors [16–19] and actuators [16–18]. CNTs are incredible structures having an array of fascinating magnetic, electrical and mechanical characteristics. The essential requirements of a good sensor are fast response, high selectivity, high volume production, low cost and high reliability.

As a sensing material, CNTs can be exploited in two different ways, for enhancing the sensitivity and selectivity. CNTs are repeatedly decorated with new elements such as metals. Conversely, CNTs can be integrated with other sensing materials, for instance, metal oxide semiconductor to enhance their sensitivity [20]. It has been established that there is a variation in electrical conductivity of conducting polymers when it is exposed to diverse organic and inorganic gases [21]. There are many conducting polymers, for instance, polyaniline (Pani), polypyrrole (PPy), polythiophene and the various derivatives of different polymers, which can be used as sensing materials [22]. Currently, many researchers tried to increase the sensitivity of CNTs-based gas sensors in various different ways, such as by depositing layers of different metals or by functionalizing with polymers [23].

In the present work, we have analysed the growth and development of single-walled carbon nanotubes-polyethylenimine (SWCNTs-PEI) functionalized-based resistive gas sensor for toxic $NO_2$ gas detection. An elaborate study of the sensor was done for various parameters such as sensitivity, reversibility and response–recovery time. We have investigated the effect of functionalization on the sensitivity of the SWCNTs-based resistive gas sensors with the polyethylenimine (PEI, Aldrich Chemicals) at room temperature.

## 2. Experimental

### 2.1 *Sensors*

The SWCNTs sensor was grown by using the standard thermal CVD method. The SWCNTs films were deposited on a $SiO_2$/Si substrate by using standard thermal chemical vapour deposition (CVD) method and co-sputtering was used for preparing the catalyst. The two planer Au electrodes were deposited on the as-grown SWCNTs surface by sputtering method followed by patterning with the standard lift-off method. The catalyst used for growing SWCNTs is achieved by co-sputtering of Fe–Mo metals (0.5 nm width) on a subsidiary cover of Al metal (10 nm width) [24]. The catalyst was annealed for 30 min in $Ar/H_2$ atmosphere at 900°C temperature. The mass flow controller was used to control the supply of carrier gas $Ar/H_2$ and the precursor gas $C_2H_2$ (acetylene) into the chamber. For SWCNTs growth, the rate of flow of $Ar/H_2$ and $C_2H_2$ gases are kept at 30 and 5 sccm, respectively, and this gas flow is maintained for 5 min. The growth pressure was maintained at 50 Torr [24]. The two planer Au electrodes were deposited on the as-grown SWCNTs surface by sputtering method followed by patterning with standard lift-off method. The sensing area comprising SWCNTs were grown by thermal CVD system on $SiO_2$/Si substrate, and the electrodes made up of gold pattern structure with 60 μm channel length was fabricated by a standard photolithography technique. The methods of physical treatment of the CNTs are not sufficiently effective, so the other option is to change the chemical properties of the surface through chemical functionalization. PEI, from Sigma Aldrich, is adsorbed on the surface of SWCNTs network by immersing in a PEI/methanol solution. The sensors were dipped for 15 min, 1 and 2 h in a 20 wt% solution of PEI polymer. The sensors are taken out from the solution and the excess PEI is removed by rinsing the sample with the methanol. So as to remove the excess methanol present over the sample, it was then heated up to a temperature of 80°C for 15 min, leaving behind a pure PEI-coated SWCNTs film without methanol.

### 2.2 *Measurements*

The PEI functionalized SWCNTs sample is placed inside a closed chamber, with one side connected to the gas distribution and the other side is open to the environment. The gas supply comes from the two gas cylinders: the first gas cylinder contains only air, while the other gas cylinder contains $NO_2$. The $NO_2$ gas (100 ppm, balanced nitrogen) used in the experiment as purchased from Linde Industrial Gases, Russia. The enclosed sample chamber also has a connection for connecting multimeter that allows recording the real-time change in the resistance of the samples when it is exposed to the $NO_2$ gases. The power density of the UV light used in the experiment is 10 W. The MKS standard mass flow controller (MFC) has been used for accurately controlling the $NO_2$ concentrations in the various ppm-levels. The schematic diagram of the setup for $NO_2$ gas sensing (figure 1). The change in the resistance of the SWCNTs sensor was recorded for various $NO_2$ gas concentrations, such as 20 and 50 ppm. In addition, to examine the repeatability of the sensor, the behaviour of the SWCNTs sensor for same $NO_2$ gas concentration was recorded for repetitive cycles. Similarly, the behaviour of PEI-doped SWCNTs sensors was also recorded in the presence of various concentrations of $NO_2$ gas and also under the same concentration of $NO_2$ gas for repetitive cycles. Inside the chamber, there is a platform for holding the gas sensor samples with two pointed electrodes, which are connected with the multimeter (UNIT-T UT803). UV light illumination is used to enhance the recovery of the gas sensor in case of

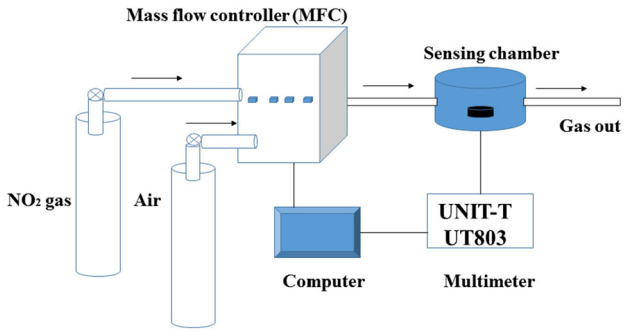


**Figure 1.** Schematic diagram of the setup for $NO_2$ gas sensing.

pristine SWCNTs sensor, whereas in case of PEI functionalized SWCNTs, we did not use UV light, hence the recovery is slow.

### 2.3 *Characterization*

A field emission electron microscopy (Nova NanoSEM 450, FEI and ZEISS sigma FESEM, India) of SWNTs-PEI as shown in figure 2 was done to study the surface morphologies, orientation and dimensions of SWNTs-PEI bilayer sensor film. The samples were mounted on the double-sided tape and the high-resolution images of SWCNTs and SWCNTs-PEI were taken as shown respectively, in figure 2a and b. In figure 2, we can see the uniform dispersion of the bilayer of SWCNTs-PEI and there are many spots which resemble island shape. The presence of cavities at the tip of the isle shaped spot helps in the adsorption of $NO_2$ molecules on the surface of the gas sensor. The PEI polymer layer essentially operates as a transitional charge transmit strip from the SWNTs to the electron acceptors. Basically, the polymer PEI accelerate the charge transfer mechanism. A lot of work has been reported, which have acknowledged the binding energy and charge transfer for $NO_2$ gas molecules [11,25]. Transmission of charged particles takes place from the surface of PEI functionalized SWCNTs to the acceptors when the $NO_2$ gas molecules are adsorbed on the surface of PEI, PEI acting as a transitional layer.

The IRS spectroscopy of the PEI-SWCNTs composites is shown in figure 3. The IR bands indicate two peaks at 1360 and 1720 $cm^{-1}$, which shows the presence of imide moieties and carbonyl in the five-membered ring structure of PEI, respectively. The strong bond at 1039 $cm^{-1}$ is the confirmatory band of the PEI polymer for its conductivity and is a measure of the degree of delocalized electrons. This bond is evident for the high conductivity, which ascribed to the C–H in-plane vibration. The bond at 1360 $cm^{-1}$ is the representative of C=C bonds, the C–C vibration occurs due to the internal defects. The other bonds observed at 2937 and 3318 $cm^{-1}$ are characteristic of C–H and O–H stretches, respectively. O–H vibrations are observed due to the amorphous carbon, which can easily form a bond with atmospheric air [26].

Raman spectroscopy (NTEGRA Spectra NT-MDT) was performed to observe the characteristic vibrational modes of SWCNTs and the subsequent effect of PEI functionalization and the spectra. Raman spectra measured on both pristine and PEI functionalized SWCNTs film is shown in figure 4. Radial breathing mode (RBM) of the sample was observed at 198 $cm^{-1}$. As the frequency of RBM is inversely proportional to the reciprocal of the diameter, it can be used to determine nanotube diameter. The RBM also provides information on chirality and thus, the electronic properties of the nanotube. Because single excitation energy was used in our experiment, only nanotubes resonant with this particular energy will demonstrate a peak at the RBM frequency. The nanotube diameter can be determined by $V_{RBM} = 248/\omega$ [27], where $V_{RBM}$ is Raman frequency shift of the RBM in $cm^{-1}$. From measured RBM, calculated SWCNT diameter is 1.25 nm. The characteristic graphene band was observed at 1590 $cm^{-1}$, the broadening of G band appeared because of the small diameter of SWCNTs. Defect-related D-band was observed at 1352 $cm^{-1}$. The low intensity of the D band signifies less number of defects in samples. Further, the decrease in the peak intensities of the functionalized SWCNTs as compared to pristine SWCNTs endorses the surface coverage by PEI on SWCNTs resulting in some modification on the surface [26].

## 3. Results and discussion

Investigations were done to understand the consequences of PEI functionalized SWCNTs gas senor samples on the $NO_2$ sensing. Figure 5 shows the sensing response and recovery curve of SWCNTs sensor towards the $NO_2$ gas molecules. Initially, when the $NO_2$ gas molecules start flowing into the closed chamber, the resistance of the sensors starts decreasing from the baseline i.e. 36.44 KΩ. However, once the analyte gas flow is stopped into the chamber, de-adsorption of the $NO_2$ molecules from the surface of SWCNTs starts taking place and consequently, causes an increase in the resistance of the sample. Many researchers have reported that due to significant binding energy at the adsorption sites, the natural recovery of the sensor is slow as compared to the response. Figure 5 explains the repeatability and recoverability in case of pristine SWCNT sensor. The major challenge faced was the recovery of the sensor. The fast recovery was accomplished by the use of UV illumination.

It is evident from figure 5 that as the $NO_2$ gas flow continues, there is a continuous decrease in the resistance of the sensor. It can also be seen that after some time, the resistance become stable and desorption of analytes takes a longer time at the ambient conditions. Therefore, to establish the decreasing curve, two different concentrations of $NO_2$ analytes were passed through the closed chamber in which the gas sensor was placed. Figures 6 and 7 show the comparison between the sensitivity of SWCNT resistive gas sensors for various

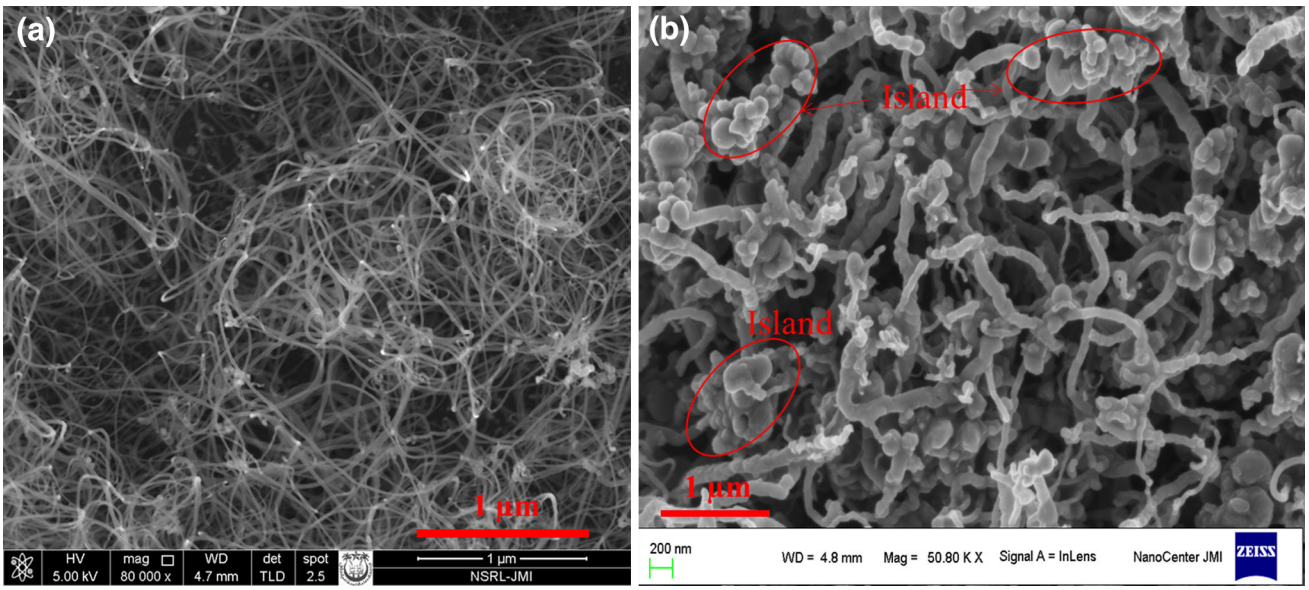


**Figure 2.** SEM micrograph of gas sensor films. (**a**) Surface micrograph of the pristine SWCNT sensor. (**b**) Surface of PEI functionalized SWCNT sensor.

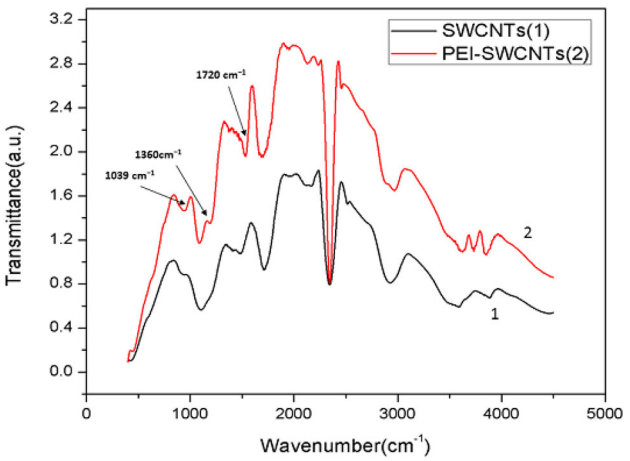


**Figure 3.** IRS spectroscopy comparison of pure SWCNTs and PEI-SWCNTs composites.

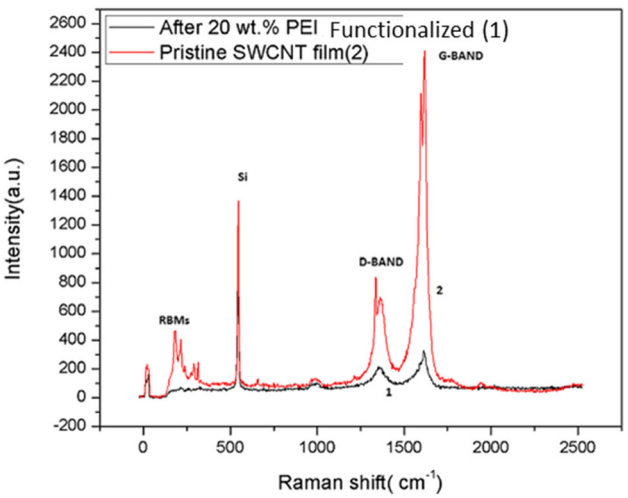


**Figure 4.** Raman spectroscopy: (1) PEI-functionalized SWCNTs sensor and (2) pristine SWCNTs sensor.

concentrations of $NO_2$ gases. It is evident from the graph that as the concentration of $NO_2$ increases correspondingly, there is an increase in response percentage. The sensitivity of chemiresistive gas sensors can be calculated as the ratio of the initial resistance of the sensor in the air to the resistance in the presence of gas.

$$S\,(\%) = (R_a - R_g)/R_a * 100, \tag{1}$$

where $S$ is the sensitivity of the gas sensor, $R_a$ the initial resistance in the presence of air and $R_g$ the final resistance in the presence of analyte gas $NO_2$.

The sensitivity of the resistive gas sensor based on SWCNTs was calculated using equation (1) and it was found to be 20.12%. The sensitivity of the SWCNTs sensor can be improved by properly functionalizing the sensor with the PEI polymer. PEI is a polymer with the repeating units of the amine group and two carbon aliphatic spacers. PEI acts as a transitional charge transfer layer from SWCNTs to the electron acceptor. There is a considerable amount of increase in the sensitivity of the gas sensor functionalized with PEI as compared to the bare CNT sensors. We have been successful in our effort to develop a PEI functionalized SWCNTs sensor with much better sensitivity. The functionalization resistive gas

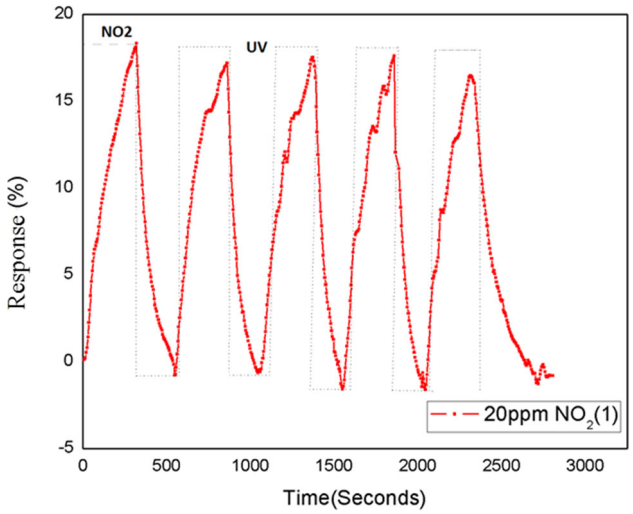


**Figure 5.** It shows the repeatability for $NO_2$ gases of the SWCNTs sensor.

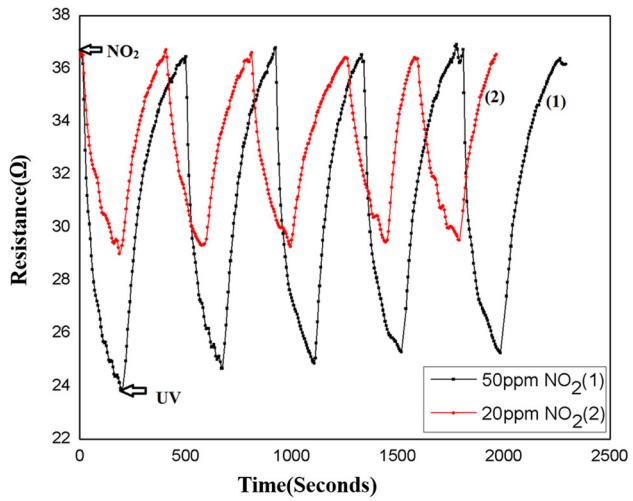


**Figure 6.** SWCNTs sensor response for various concentrations of $NO_2$ gases, such as 20 and 50 ppm.

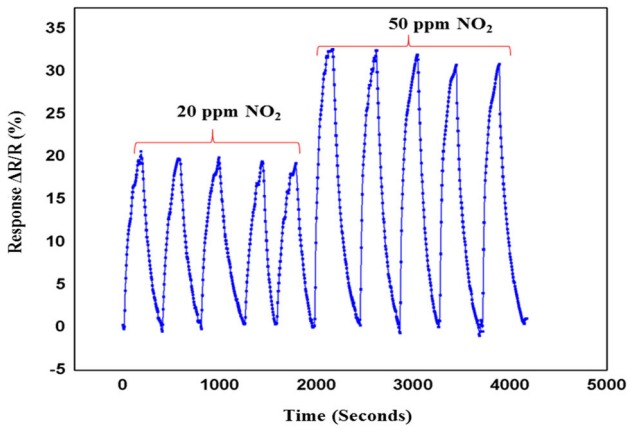


**Figure 7.** Response $\Delta R/R$ (%) for various concentrations of $NO_2$ gases, such as 20 and 50 ppm.

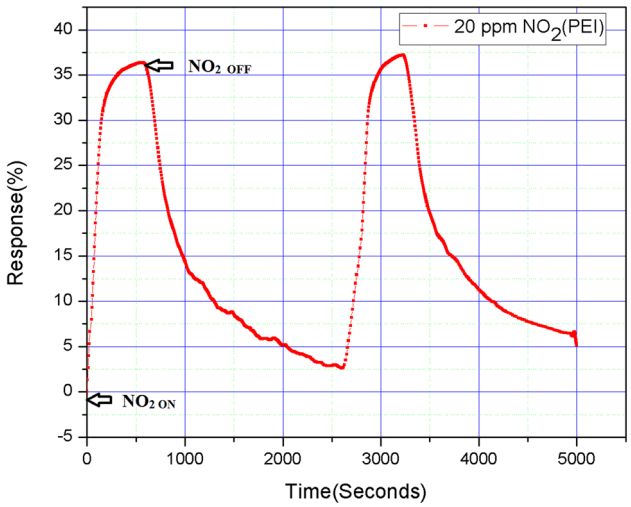


**Figure 8.** Response of PEI-functionalized SWCNTs resistive gas sensor in the presence of $NO_2$ gases.

sensor based on SWCNTs has shown a substantial increase in the sensitivity and was found as 37.00% for 20 ppm $NO_2$ gas detection. The semiconducting pristine SWCNTs sensor shows p-type behaviour prior to PEI functionalization and it can be corroborated with the decrease in the resistance in the presence of $NO_2$ gas. The adsorption of PEI on the sidewalls of SWCNTs after functionalization is irreversible and it cannot be completely removed even after extensive rinsing in ethanol. This is in complete agreement with the other recent findings of the irreversible polymer wrapping around SWCNTs [28–30]. So, to control the functionalization level of SWCNTs network, the sensors were immersed in a solution of 20 wt% PEI/methanol for 15 min, 1 and 2 h, respectively. There was a substantial increase in the sensitivity of the modified sensor. It was found that the initial resistance of the sensors kept on increasing as the sensors were immersed for a longer time. This behaviour can be due to the donor effect of PEI on the p-type of SWCNT channel. The results concur with the first observation; this tendency is presumably by the virtue of accumulation of extra acceptor molecules resulting from the PEI functionalization of the SWCNTs surface of the gas sensors. There is a decrease in the channel resistance of p-type of SWCNTs because $NO_2$ acts as electron acceptors.

The response of the SWCNT sensor in the presence of $NO_2$ gas was found to be 20.12%. On the other hand, when the SWCNT sensor was functionalized with PEI polymer, then, the response of the doped SWCNT sensor increased up to 37% as shown in figure 8. The charge transfer takes place from the SWNT surface to the $NO_2$ gas molecules with PEI polymer acting as an intermediate layer. An efficient molecular photodesorption of $NO_2$ gas from the surface of SWCNTs in the presence of UV illumination is achieved [31,32]. A comparison table comparing the performance of the developed sensor

**Table 1.** Comparison of different materials based on $NO_2$ gas sensor performances.

| Materials | $NO_2$ concentration | Sensitivity/response (%) | Response time | Operating temperature (°C) | References |
|---|---|---|---|---|---|
| ZnO | 1–30 ppm | 3.3 | 25 s | 250 | [40] |
| Silicon/ZnO | 200 ppb | 35 | 50 s | 25 | [41] |
| $MoS_2$−Au | 2.5 ppm | 30 | 4 min | RT | [42] |
| RGO−$MoS_2$−CdS | 0.2 ppm | 27.4 | 25 s | 75 | [43] |
| $MoS_2$/ZnO NWs | 50 ppm | 31.2 | 5 min | 200 | [44] |
| $MoS_2$/PSi NWs | 50 ppm | 28.4 | — | RT | [45] |
| F-SWCNTs/Ps | — | 36 | 11 s | RT | [46] |
| SWCNTs/Ps | — | 13.5 | 13 s | 100 | [46] |
| F-SWCNTs | 50 ppm | 37 | 4 min | RT | This work |

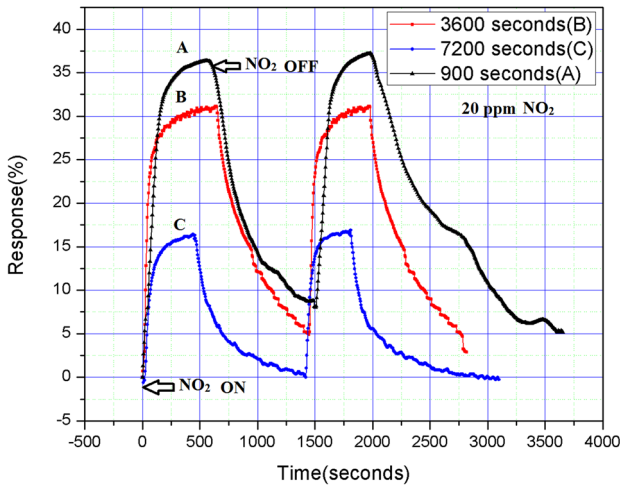


**Figure 9.** Comparison of PEI-functionalized SWCNTs sensor response for the various durations of immersion of sensor in PEI/methanol solution.

with the other sensors developed for $NO_2$ gas sensing has been included and shown in table 1.

At atmospheric conditions, the nature of SWCNTs is p-type [33–35]. In the case of pristine SWCNTs, when $NO_2$ gas interacts with SWNTs, the gas molecules withdraw electron and thus, increases the majority carriers, which decreases the resistance strenuously [36,37]. The strong carbon–carbon bonding in CNTs suppresses their reactivity and limits their sensing capability. Structural defects increase the chemical reactivity of carbon nanotubes [38,39]. Pristine SWCNTs have fewer defects and hence, only a small number of gas molecules adsorbed on the surface during exposure. During the PEI functionalization process, additional defects (removal of carbon atoms, breaking of C=C bonds) are created on the sidewalls as well as on the ends of SWCNTs. Functional groups, such as amine groups are preferably attached to these defects sites, which further facilitates the adsorption of $NO_2$ gas molecules. As a result, more $NO_2$ gas molecules are adsorbed on the SWCNTs sensor, contributing to increased charge transfer between CNTs and $NO_2$ gas molecules. This results in a large change in the resistance of the sensor. Thus, the sensitivity of the PEI functionalized SWCNTs $NO_2$ gas sensor is enhanced. Also, the degree of enhancement in the sensitivity of SWCNTs depends on the type of functional group and the amount of functional group attached. The influence of moisture on the actual gas sensing response is found to be insignificant. The exposure of relative humidity (RH) does not make any sensible change in the baseline resistance of the sensor. We performed our experiments at 5, 10, 20 wt% of PEI. Our sensor gave the best result for 20 wt% of PEI.

However, as the immersion duration of SWCNT sensor into the PEI/methanol solution increases sensitivity, and recoverability of the sensor decreases as shown in figure 9. There are two proposed reasons for the decrease in sensitivity and recoverability. The first reason is the accumulation of PEI polymer layer on the surface of SWCNTs after long hours of immersion. This deposition of a thick layer of PEI on the SWCNT surface decreases the sensitivity of SWCNT by reducing the charge transfer between the SWCNT layer and $NO_2$ molecules as shown in figure 9.

## 4. Conclusion

We have developed a chemiresistive SWCNTs-PEI functionalized gas sensor by using a thermal CVD method. The higher adhesive coefficient for the electron-withdrawing $NO_2$ of PEI-coated SWCNTs than untreated SWCNTs. At room temperature, PEI-SWCNTs-coated resistive gas sensor demonstrated elevated sensing behaviour and swift reaction to $NO_2$. Furthermore, owing to room temperature operation of the resistive gas sensor can be encouragingly exploited in the environment observation. A detector was successfully developed to detect low concentration (ppm) of $NO_2$ and by an accurate selection of thermal treatment, the complete recovery of the sensor was achieved. More importantly, it was found that with the increase in the duration of functionalization, the sensitivity of the SWCNTs is enhanced. By controlling

the basicity and the functionalization concentration of SWCNTs network, the PEI-SWCNT sensors can be extended to various domains and the selectivity of the sensor can be configured based on various chemical environments. The achieved results are important as they demonstrate that the sensitivity of an SWCNTs gas sensor can be enhanced by the presence of attached amine group. However, apart from sensitivity, selectivity is also a challenge for a reliable CNT gas sensor development. As $NO_2$ gas sensors are intended to be deployed in both open and closed environments, the study of the effect of temperature and humidity is very important for calibration, interface circuitry and working room temperature SWCNT nitrogen dioxide sensor device. The optimization of the resistive gas sensor based on SWCNTs would be examined profoundly in future analysis.

## Acknowledgements

The investigation was supported by the Ministry of Science and Higher Education of Russian Federation (project 0777-2017-0009).

## References

[1] WHO 2016 WHO releases country estimates on air pollution exposure and health impact, *WHO*, Online. Available: http://www.who.int/mediacentre/news/releases/2016/air-pollution-estimates/en/#
[2] Pan X, Zhao X, Bermak A and Fan Z 2016 *IEEE Electr. Dev. Lett*. **37** 92
[3] Cullinan P, Muñoz X, Suojalehto H, Agius R, Jindal S, Sigsgaard T *et al* 2017 *Lancet Resp. Med*. **5** 445
[4] Liddle L, Monaghan C, Burleigh M C, McIlvenna L C, Muggeridge D J and Easton C 2018 *Nitric Oxide Biol. Chem*. **72** 59
[5] Antisari M V, Marazzi R and Krsmanovic R 2003 *Carbon NY* **41** 2393
[6] Teymourzadeh M and Kangarlou H 2012 *World Appl. Sci. J*. **18** 879
[7] Lee A P and Reedy B J 1999 *Sensors Actuators B Chem*. **60** 35
[8] Martinelli E, Polese D, Catini A, Amico A D and Di Natale C 2012 *Sensors Actuators B Chem*. **161** 534
[9] Wei B Y, Hsu M C, Su P G, Lin H M, Wu R J and Lai H J 2004 *Sensors Actuators B Chem*. **101** 81
[10] Van Hieu N, Thuy L T B and Chien N D 2008 *Sensors Actuators B Chem*. **129** 888
[11] Ghoorchian A and Alizadeh N 2018 *Sensors Actuators B Chem*. **255** 826
[12] Sayago I, Fernández M J, Fontecha J L, Horrillo M C, Vera C, Obieta I *et al* 2012 *Sensors Actuators B Chem*. **175** 67
[13] Iijima S 1991 *Nature* **354** 56
[14] Abdulla S, Mathew T L and Pullithadathil B 2015 *Sensors Actuators B Chem*. **221** 1523
[15] Chen L, Chen Z, Huang Z, Huang Z, Wang Y, Li H *et al* 2015 *J. Phys. Chem. C* **119** 28757
[16] Shen J, Zhu Y, Yang X and Li C 2012 *Chem. Commun*. **48** 3686
[17] Yamada T, Hayamizu Y, Yamamoto Y, Yomogida Y, Izadi-Najafabadi A, Futaba D N *et al* 2011 *Nat. Nanotechnol*. **6** 296
[18] Lipomi D J, Vosgueritchian M, Tee B C K, Hellstrom S L, Lee J A, Fox C H *et al* 2011 *Nat. Nanotechnol*. **6** 788
[19] Rafiee M, Rafiee J, Wang Z, Song H, Yu Z and Koratkar N 2009 *ACS Nano* **3** 3884
[20] Balint R, Cassidy N J and Cartmell S H 2014 *Acta Biomater*. **10** 2341
[21] Inoue S and Matsumura Y 2009 *Chem. Phys. Lett*. **469** 125
[22] Lupi C, Felli F, Brotzu A, Caponera M A and Paolozzi A 2008 *IEEE Sensors J*. **8** 1299
[23] Körösi L, Mogyorósi K, Kun R, Németh J and Dékány I 2004 *Prog. Colloid Polym. Sci*. **125** 27
[24] Mishra P, Harsh H and Islam S S 2013 *Int. Nano Lett*. **3** 46
[25] Battie Y, Ducloux O, Thobois P, Dorval N, Lauret J S and Loiseau A 2011 *Carbon* **49** 3544
[26] Hussain S, Jha P, Chouksey A, Raman R, Islam S S, Islam T *et al* 2011 *J. Mod. Phys*. **2** 538
[27] Jorio A, Saito R and Hafner J H 2001 *Phys. Rev. Lett*. **86** 6
[28] Kong J and Dai H 2001 *J. Phys. Chem. B* **105** 2890
[29] Shim M, Javey A, Kam N W S and Dai H 2001 *J. Am. Chem. Soc*. **123** 11512
[30] Connell M J O, Boul P, Ericson L M, Hu C, Wang Y, Haroz E *et al* 2001 *Chem. Phys. Lett.* **342** 265
[31] Karthigeyan A, Minami N and Iakoubovskii K 2008 *Jpn. J. Appl. Phys*. **47** 7440
[32] Jeon J Y, Kang B C, Byun Y T and Ha T J 2019 *Nanoscale* **11** 1587
[33] Fukumaru T, Fujigaya T and Nakashima N 2015 *Sci. Rep*. **5** 1
[34] Geier M L, McMorrow J J, Xu W, Zhu J, Kim C H, Marks T J *et al* 2015 *Nat. Nanotechnol*. **10** 944
[35] Takenobu T, Takano T, Shiraishi M, Murakami Y, Ata M, Kataura H *et al* 2003 *Nat. Mater*. **2** 683
[36] Kumar D, Kumar I, Chaturvedi P, Chouksey A, Tandon R P and Chaudhury P K 2016 *Mater. Chem. Phys*. **177** 276
[37] Evans G P, Buckley D J, Skipper N T and Parkin I P 2014 *RSC Adv*. **4** 51395
[38] Terrones M and Terrones H 1996 *Fullerene Sci. Technol*. **4** 517
[39] Crespi V H, Cohen M L and Rubio A 1997 *Phys. Rev. Lett*. **79** 2093
[40] Chen X, Shen Y, Zhang W, Zhang J, Wei D, Lu R *et al* 2018 *Appl. Surf. Sci*. **435** 1096
[41] Betty C A, Sehra K, Barick K C and Choudhury S 2018 *Anal. Chim. Acta* **1039** 82
[42] Yong Zhou Y G, Cheng Z and Xiaogang L 2018 *Appl. Phys. Lett*. **113** 082103
[43] Shao S, Che L, Chen Y, Lai M, Huang S and Koehn R 2019 *J. Alloys Compd*. **774** 1
[44] Zhao S, Wang G, Liao J, Lv S, Zhu Z and Li Z 2018 *Appl. Surf. Sci*. **456** 808
[45] Zhao S, Li Z, Wang G, Liao J, Lv S and Zhu Z 2018 *RSC Adv*. **8** 11070
[46] Naje A N and Mahmood W K 2018 *IOP Conf. Ser. Mater. Sci. Eng*. **454** 1